Materials Letters 100 (2013) 180–183

Contents lists available at SciVerse ScienceDirect

Materials Letters

journal homepage: www.elsevier.com/locate/matlet

Fe-catalyzed thermal conversion of sodium lignosulfonate to graphene

Sung Phil Mun [a], Zhiyong Cai [b], Jilei Zhang [c,*]

[a] Department of Wood Science and Technology, Chonbuk National University, Jeonju, Jeonbuk 561-756, South Korea
[b] Forest Products Laboratory, USDA Forest Service, One Gifford Pinchot Drive, Madison, WI 53726-2398, USA
[c] Department of Forest Products, Mississippi State University, MS State, MS 39762-9820, USA

ARTICLE INFO

Article history:
Received 14 January 2013
Accepted 26 February 2013
Available online 7 March 2013

Keywords:
Lignosulfonate
Sulfite pulping
Fe nanoparticles
Graphene
Thermal treatment
Raman spectrum

ABSTRACT

Sodium lignosulfonate (LS) from sulfite pulping processing was used as a carbon source to synthesize graphene. LS was mixed with Fe nanoparticles (FeNPs) as a catalyst and thermally treated at 1000 °C for 1 h. The Raman spectrum and X-ray diffraction pattern suggested that graphene sheets were formed in LS thermally treated with FeNPs (Fe-HTLS). Scanning electron microscopy image of Fe-HTLS showed clusters of thin graphene sheets appearing in the form of nanoflowers. High-resolution transmission electron microscopy and electron reflection images provided further evidence of the formation of graphene in LS thermally treated in the presence of Fe catalyst.

1. Introduction

Lignin is a renewable carbon source and the second most abundant biopolymer next to cellulose on earth. It is a cross-linked and complex natural polymer composed of phenylpropane unit as a basic unit. Its complex structure makes the production of value-added chemicals from lignin difficult. A great amount of lignin can be obtained from the pulping industry in the name of kraft lignin (or thiolignin) and lignosulfonate (LS). The approximate amount of lignin production in the existing pulping industry worldwide is estimated at more than 50 million tons/year [1]. However most lignin is not isolated, especially in the kraft pulp mills which are 95% of the world production market, but is burned onsite to recover pulping chemicals and provide steam for power production. Therefore, commercially available lignin in the market is mostly LS from the sulfite pulping process. The global production of LS is currently around 1 million tons/year [1]. LS has been used for concrete admixtures, dispersants and dust suppression for roads, pellet binders, and vanillin [2]. Although many trials have been made to convert lignin into value-added materials, so far there are few reports on the successful commercialization of lignin-related products. If lignin, the by-product from current pulping and bio-ethanol processes, can be an alternative carbon source for the production of high-value carbon-based nanomaterials, it would be an incentive for the further utilization of lignin. However, to our knowledge, there are no systematic approaches in the processing of lignin for conversion into carbon-based nanomaterials, and there is no report on the efficacious conversion of lignin to graphene. The objective of this study was to explore whether LS, an inexpensive feedstock, can be easily converted to carbon nanomaterials such as graphene under simple thermal treatment conditions in the presence of Fe nanoparticles (FeNPs) as a catalyst.

2. Experimental

Materials: LS (Na salt), from Sigma-Aldrich Inc. (St. Louis, MO, USA), was used as a carbon source. FeNPs (25 nm in average particle size), from Sun Innovations Inc. (Fremont, CA, USA), were used as the catalyst for the thermal treatment.

Thermal treatment: Thermal treatment of LS was carried out in a split-hinge 2 in.-quartz tube electric furnace (Lindberg/Blue M 1200) equipped with a temperature controller (Lindberg/Blue UTC 150). The quartz tube had an outer diameter of 2 in. and a length of 32 in. For each experimental run, 250 mg of FeNPs (1 part by weight) and 1000 mg of LS (4 parts by weight) were mixed and then ground in an agate mortar. The well-ground sample mixture was loaded into a porcelain boat which was placed in the middle of the quartz tube. The sample was heated to 1000 °C at a ramping rate of 20 °C/min under argon with a flow rate of 1 L/min. The temperature was held at 1000 °C for 1 h, and the furnace then was turned off and the sample cooled to ambient temperature under argon atmosphere.

LS samples after thermal treatment contained the inorganic ash that originated from the pulping chemicals. The ash may

* Corresponding author. Tel.: +1 662 325 9413; fax: +1 662 325 8126.
E-mail address: jzhang@cfr.msstate.edu (J. Zhang).

0167-577X/$ - see front matter © 2013 Elsevier B.V. All rights reserved.
http://dx.doi.org/10.1016/j.matlet.2013.02.101

disrupt instrumental characterization of the samples and make data analyses difficult. To remove the water soluble inorganic ash from the thermally-treated LS sample, 500 mg of the thermally-treated LS sample and 20 mL of de-ionized water (DI-water) were added to a flask, and the mixture boiled for 30 min. The boiled sample was filtered through a nylon membrane (0.45 μm) and then rinsed with 100 mL of DI-water. The washed sample was dried in oven at 105 °C overnight.

Characterization: Raman spectra were recorded at three locations of each sample using a Jobin Yvon LabRam HR spectrometer (Horiba) with a 514.56 nm Ar laser. Powder X-ray diffraction (XRD) was performed with a Rigaku SmartLab X-ray diffractometer (Rigaku) using Cu Kα radiation ($\lambda = 1.5418$ Å). Field emission scanning electron microscopy (FE-SEM) images were obtained by a JSM-6500F (JEOL). For high-resolution transmission electron microscopy (HRTEM), the samples were further ground in ethanol by an agate mortar to reduce their size and then a drop of this suspension was dripped onto a 300 mesh copper grid with a holey support film. HRTEM analysis was performed on a JEM 2100F (JEOL) equipped with an EDAX (Ametek).

3. Results and discussion

Table 1 shows the result of carbonization yields of LS thermally-treated with Fe (Fe-HTLS) as the catalyst and LS thermally-treated without Fe catalyst (HTLS). The carbonization yields of Fe-HTLS and HTLS were 50.1% and 45.3%, respectively. In the case of Fe-HTLS, as FeNPs were added to LS as the catalyst the weight of FeNPs needs to be deducted from the total weight of the LS and FeNPs mixture to calculate the true carbonization yield of LS. The carbonization yield of LS thermally-treated with Fe after the weight correction of FeNPs was 30.2%. On the other hand, an ash content of 19.5% was assumed in the thermally treated LS. This content was determined using the TAPPI Standard T 211-om 93. Therefore, the carbonization yields of Fe-HTLS and HTLS after ash weight correction were 24.3% and 36.5%, respectively. The lower carbonization yield of Fe-HTLS may be due to the excessive decomposition of LS by the catalytic action of FeNPs.

Raman spectroscopy is an effective technique to characterize carbon structures of carbonaceous materials such as graphite, graphene, carbon nanotubes, and diamond-like carbon [3–8]. Therefore, any significant changes in the chemical structure of LS which occurred during the thermal treatment were characterized by Raman spectroscopy. Fig. 1 shows Raman spectra of HTLS and Fe-HTLS. The Raman spectra in both samples show two distinct peaks, G and D peaks, that appear around 1580 and 1350 cm^{-1}, respectively. In general, the D peak indicates the vibration of sp^2-hybridized carbon bonded with structural imperfections while the G peak indicates the in-plane vibration of sp^2-bonded crystalline carbon [3,9,10]. Thus, the G peak in Fig. 1 indicates that graphite- or graphene-like carbon structures may be formed in both samples, while the D peak indicates a decrease

Table 1
Carbonization yields after thermal treatment of LS with and without Fe nanoparticles, and the yields after the correction of Fe nanoparticles and ash in Fe-HTLS and HTLS.

Sample	Carbonization yield (%)		
	After thermal treatment	After correcting for FeNPs	After correcting for ash
Fe-HTLS	50.1	30.2	24.3
HTLS	45.3	–	36.5

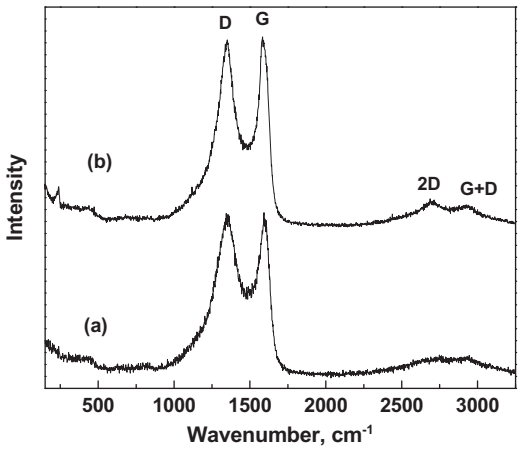

Fig. 1. Raman spectra of LS thermally treated without Fe nanoparticles (a) and with Fe nanoparticles (b).

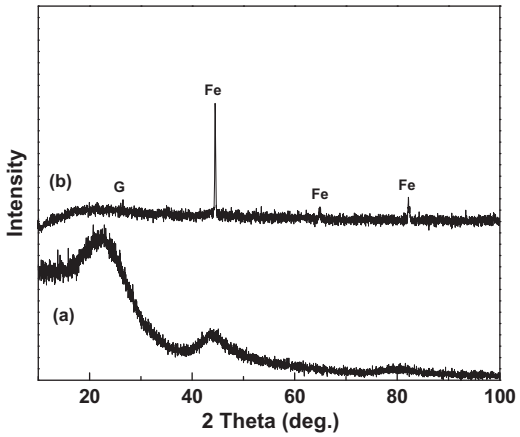

Fig. 2. Powder X-ray diffraction patterns of LS thermally treated without Fe nanoparticles (a) and with Fe nanoparticles (b), G: graphite, Fe: iron.

of the size of the in-plane sp^2 domains as well as an increase of edge planes and the degree of disorder in both samples. In the Raman spectrum of Fe-HTLS, the width of the D peak is narrower than HTLS, which indicates that Fe-HTLS samples contain less structural imperfections than that in HTLS samples. In addition, the peak intensity ratio of the D″ peak (1500–1550 cm^{-1}, associated with an amorphous sp^2-bonded carbon [9]) to the G peak, $I_{D''/G}$, as a carbonization indicator, decreased from 0.49 to 0.38 with Fe. The lower peak intensity ratio indicates that Fe catalyst reduced the structural imperfections and amorphous phase for sp^2-bonded carbon [3,9]. On the other hand, Fe-HTLS had a 2D peak other than D and G peaks on the spectrum. The 2D peak (also called the G′peak) is the second order of the D peak [4]. The width of the 2D peak ranged from 2650 to 2750 cm^{-1}, which corresponded to the turbostratic graphite [8] with its graphene layers stacking in a randomly rotated fashion with respect to one another along the *C*-axis [4]. Thus, graphene sheets may have occurred in Fe-HTLS samples, but they mostly exist in the form of overlapped graphenes with a turbostratic structure.

For further analysis of the structural difference between Fe-HTLS and HTLS samples, their XRD patterns were measured (Fig. 2). In general, the XRD pattern of graphite powder (including artificial graphite and meso carbon microbeads) exhibits a sharp and characteristic peak (002) of graphite at 26–27° [5,6,11]. HTLS had two dispersive and broad diffraction peaks at 26° and 43° on its XRD spectrum as shown in Fig. 2(a). These two peaks correspond to (002) and (100) planes of graphite [9]. The high

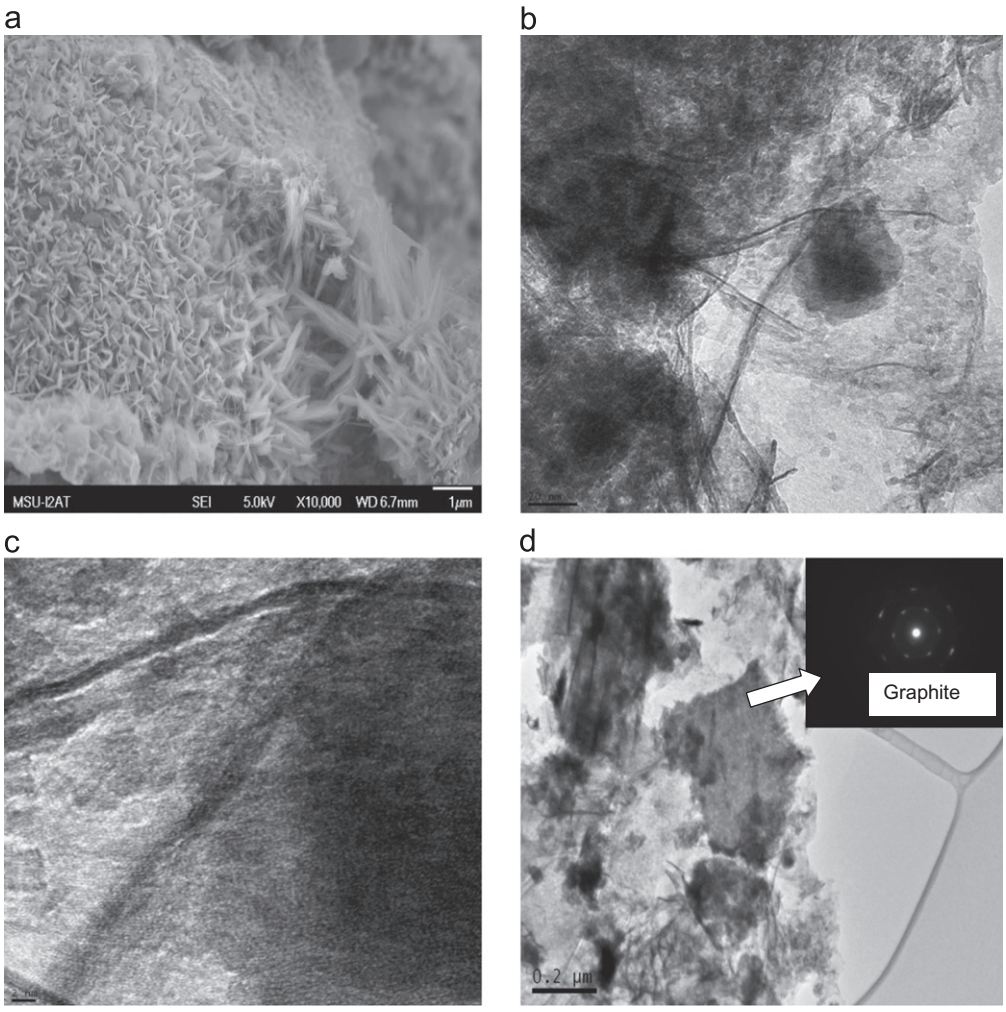

Fig. 3. SEM and HRTEM images of graphene nanosheets of LS thermally treated with Fe nanoparticles: (a) a SEM image exhibiting clusters of graphene nanosheets in the form of nanoflowers, (b) and (d) typical HRTEM images presenting folded and wrinkled graphene nanosheets, and (c) a HRTEM image in the center of (b). The inset (d) shows an electron diffraction pattern of graphite.

intensity in the range of 10–25° indicates that HTLS contains a significant amount of amorphous carbon in agreement with Raman spectroscopy. In the case of Fe-HTLS, the two peaks corresponding to graphite did not appear on its XRD spectrum as shown in Fig. 2(b), only typical iron lattices. Some studies have reported that the structural change from graphite to graphene sheets causes a weakened (002) peak of graphene sheets [5,6,11]. In addition, this phenomenon may also occur due to the strong intensity of the iron peaks on the XRD spectrum. Based on the results of Raman spectroscopy and XRD, we expected that graphene nanosheets may be formed in Fe-HTLS samples. To verify this, the morphology and nanostructure of Fe-HTLS were characterized by SEM and HRTEM observations.

Fig. 3(a) shows the SEM image of Fe-HTLS sample surface. The surface was covered with "flower-like" graphene sheet agglomerate. Fig. 3(b) is a typical HRTEM image of Fe-HTLS samples showing that graphene sheets are wrinkled and folded like crumpled paper. Fig. 3(c), a higher magnification image of the center part of Fig. 3(b), shows well-ordered graphene surface. The inset of Fig. 3(d) exhibits a typical sixfold symmetry electron pattern for graphite [12]. Some researchers [13,14] reported that when wood char is thermally treated at the same temperature of this study in the presence of Fe catalyst the majority of carbon nanomaterials formed were carbon-encapsulated Fe nanoparticles with well-aligned multi-graphitic layers and also graphitic carbon structures with long and entangled multi-layers. However, in this study graphene nanosheets are the dominantly formed carbon nanomaterials.

The graphitization is preceded with the transformation of sp^3 hybridized to sp^2 carbon atoms. In the case of wood, the major component is carbohydrates such as cellulose and hemicellulose that account for 70–80% of wood, and these carbohydrates are mostly composed of sp^3 hybridized carbon atoms. Therefore the conversion of sp^3 hybridized carbon atoms to sp^2 hybridized carbon atoms must occur in the graphitization process and the process usually requires a high temperature more than 1400 °C [9,15,16]. However, lignin basically has a sp^2 bonded aromatic ring structure that makes the conversion of lignin to graphene nanosheets much easier than that of wood carbohydrates, especially in the presence of Fe catalyst. Ishimura et al. [9] reported that the carbonized wood at 1800 °C has more disordered carbon crystallites than the carbonized organosolve lignin.

4. Conclusions

This study demonstrated that graphene nanosheets can be prepared from technical sodium lignosulfonates by a simple thermal treatment in the presence of Fe catalyst. Although further studies are needed for this graphene synthesis method, this study suggested a possibility that lignin can be a unique valuable carbon source for the synthesis of graphene.

Acknowledgments

This work was supported by the USDA Forest Service through Grant no. 11JV11111124097111121332. The authors would like to acknowledge Dr. Fumiya Watanabe (Nanotechnology Center, the University of Arkansas at Little Rock) in taking the high resolution TEM images and Dr. Shane C. Street (University of Alabama) for allowing us to use the FT-Raman spectrophotometer. This manuscript was approved for publication as Journal Article no FP 667 of the Forest and Wildlife Research Center, Mississippi State University.

References

[1] Gosselink RJA, Jong Ede, Guran B, Abächerli A. Ind Crops Prod 2004;20:121–9.
[2] Sjöström E. Wood chemistry: fundamentals and applications. 2nd ed. Academic Press; 1993, p. 239-240.
[3] Yamauchi S, Kurimoto Y. J Wood Sci 2003;49:235-240.
[4] Hojati-Talemi P, Simon GP. Carbon 2010;48:3993–4000.
[5] Lian P, Zhu X, Liang S, Li Z, Yang W, Wang H. Electrochim Acta 2010;55:3909–14.
[6] Kong Y, Zhao D-L, Bai L-Z, Shen Z-M. Mater Lett 2011;65:2739–41.
[7] Wang B, Park J, Su D, Wang C, Ahn H, Wang G. J Mater Chem 2012;22:15750–6.
[8] Dresselhaus MS, Jorio A, Hofmann M, Dresselhaus R. Nano Lett 2010;10:7518.
[9] Ishimaru K, Hata T, Bronsveld P, Nishizawa T, Imamura Y. J Wood Sci 2007;53:442–8.
[10] Ishimaru K, Hata T, Bronsveld P, Meier D, Imamura Y. J Mater Sci 2007;42:122–9.
[11] Guo P, Song H, Chen X. Electrochem Commun 2009;11:1320–4.
[12] Wu NJ, Ignatiev A. Phys Rev B 1982;25:2983–6.
[13] Du Y, Wang C, Toghiani H, Cai Z, Liu X, J. Zhang, et al., For Prod J 2010;60:527–33.
[14] Mun SP, Cai Z, Watanabe F, Agarwal UP, Zhang J. For Prod J 2012;62:462–6.
[15] Byrne CE, Nagle DC. Carbon 1977;35:267–73.
[16] Hata T, Yamne K, Kobayashi E, Imamura Y, Ishihara S. J Wood Sci 1988;44:332–4.